Available online at www.sciencedirect.com

ScienceDirect

Procedia CIRP 85 (2019) 121–126

www.elsevier.com/locate/procedia

2nd CIRP Conference on Composite Material Parts Manufacturing (CIRP-CCMPM 2019)

Production of Hybrid Tubular Metal-Fiber-Preforms: Material Characterization of Braided Hoses with a Binder

Paul Ruhland[a,*], Manuel Berger[a], Sven Coutandin[a], Jürgen Fleischer[a]

[a]*Karlsruhe Institute of Technology, wbk Institute of Production Science, Kaiserstr. 12, 76131 Karlsruhe, Germany*

* Corresponding author. Tel.: +49 721 608-47357; fax: +49 721 608-45005. *E-mail address:* paul.ruhland@kit.edu

Abstract

Hybrid shafts or rods, where the area of load introduction is metallic (e.g. steel or aluminium) and the area of load transfer is made of fibre reinforced plastics (FRP), are an established concept for lightweight parts. Besides the monolithic FRP and the metallic areas, the overlap area of both materials is particularly important. Such parts can beneficially be produced by the use of liquid composite moulding (LCM), where the bonding process takes place during the resin curing. This is called intrinsic hybridization. Beforehand it is crucial to produce a near-net-shape preform in which the metallic end fittings for the load introduction are already integrated. To manufacture such parts constantly with a high quality, a process model of the joining by draping the braided preform is necessary.

In this paper an approach for the production of hybrid preforms made of braided hoses and metallic fittings is presented in order to develop a process model. The process starts with a cylindrical multi-layer preform made of braided hoses, in which the layers are bonded by a thermoplastic binder powder. The decisive process step is the draping of the preform onto the metallic fitting. For this forming step, the material characterization of the hybrid preform plays an important role. Several material tests to determine the textile parameters of the preform are therefore evaluated and performed. Finally, the results of these tests are presented and discussed.

Keywords: Fiber Reinforced Plastic; Material; Preform

1. Introduction

Lightweight shafts or rods have many fields of application. In aviation, lightweight drive shafts may be used in turbines. Tension rods are used for the actuation of landing flaps. In the ship industry, steel drive shafts may be replaced by lightweight shafts to save weight and improve the vibrational behavior. Tension rods also exist in the steering system in the automotive industry, where lightweight drive shafts are presented for both electric and conventional propulsion systems.

In all above-mentioned applications, lightweight shafts or rods made of fiber reinforced plastics (FRP) have a very high potential to save weight, since the load direction in these parts is usually uniform.

Introducing loads into the FRP shafts or rods is particularly challenging since the FRP has disadvantages in tribological contact and under multiaxial stresses. A possible solution lies in the usage of hybrid parts, where the load introduction is made of metal and the load transfer region is made of FRP [1].

In the past years, numerous approaches on the manufacture of hybrid metal-FRP shafts or rods have been presented. These manufacturing processes can generally be divided into two main groups: intrinsic and extrinsic hybridization. By definition, intrinsic hybridization describes a joining process of two components whose materials are connected by primary shaping or by forming one of the components. In contrast to extrinsic hybridization processes, no subsequent joining process is necessary [1].

Established processes for intrinsic hybridization of metallic end fittings with FRP shafts or rods are integral blow molding for both axial forces (tension rods) as well as torques (drive shafts) [2] and the pin technology, where small pins are welded onto the end fitting and then over-braided or over-winded [3].

10.1016/j.procir.2019.09.013

A new process for producing such parts is the rotational molding process [4]. Here, the infiltration of the preform with resin is supported by centrifugal forces: Preform and metallic end fitting are put into a two-shell mold which is subsequently closed. Then, the tool starts rotating around the axial axis. Resin is filled in the cavity inside of the preform. Due to the centrifugal forces, the resin infiltrates the preform and hardens while rotating, so that the metallic end fittings are joined intrinsically to the FRP.

The infiltration of pure cylindrical overlap areas between the FRP and the metal has been described by Koch in [5], while the infiltration of undercut geometries in axial direction is still a focus of research. Undercut geometries in the overlap area have the potential to transfer higher loads due to the form fit compared to a cylindrical shape with only adhesive bonding [2]. To manufacture such undercut parts, the preform needs to be draped near-net-shape onto the metallic end fitting. Otherwise, resin pockets and not-infiltrated fibers would lower the quality and the performance of the hybrid part significantly.

At present, there is no process chain for producing hybrid fiber-metal preforms. Thus, this paper addresses two objectives: First, an overall process chain for producing hybrid preforms is presented, from braiding up to hybrid preforming. Second, the material characterization of the braided sleeves is described, which constitutes the basis for the design of the process by developing a process model in finite element simulation.

2. Approach: Process Chain for Hybrid Preforms

The process chain for the production of hybrid preforms is divided into two main manufacturing process steps (see also Fig. 1):

1.) *Monolithic preforming*: A monolithic cylindrical preform consisting of multiple braided layers and stabilized by a thermoplastic binder is manufactured.

2.) *Hybrid preforming*: The monolithic preform is joined with the metallic end-fittings and near-net-shape draped to form a hybrid preform.

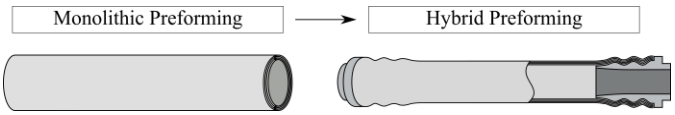

Fig. 1: Main process steps for manufacturing hybrid preforms

Monolithic Preforming

Two different processes, as shown in Fig. 1, can be used for the manufacturing of the monolithic preform. The first option constitutes in manufacturing the monolithic preform by quasi-endless over-braiding. Here, a braided sleeve is manufactured. Afterwards, a binder powder is applied onto the quasi-endless sleeve. This binder-applied sleeve is then over-braided with another layer of endless fibers. Subsequently, the binder powder is activated (e.g. by heat). These steps are repeated until the preform consists of the necessary number of layers. The now quasi-endless preform is then cut into the needed lengths for the application to form the monolithic preform.

The other option constitutes in manufacturing the monolithic preform by a subsequent stacking of layers, which is also exemplary described in [6] for hybrid yarns. In this paper, a (quasi-) endless braided sleeve is cut into pieces which have the length of the final application. These pieces are then widened and stacked over each other to form a multiple layer preform. In between the stacking steps of each layer, a binder powder is applied onto each layer and activated.

These steps are repeated until the preform consists of the necessary number of layers. Finally, the edges of the preform are cut to avoid fiber misalignments and form the monolithic preform.

For producing cylindrical monolithic preforms, the following subsequent process steps have the greatest impact on quality:

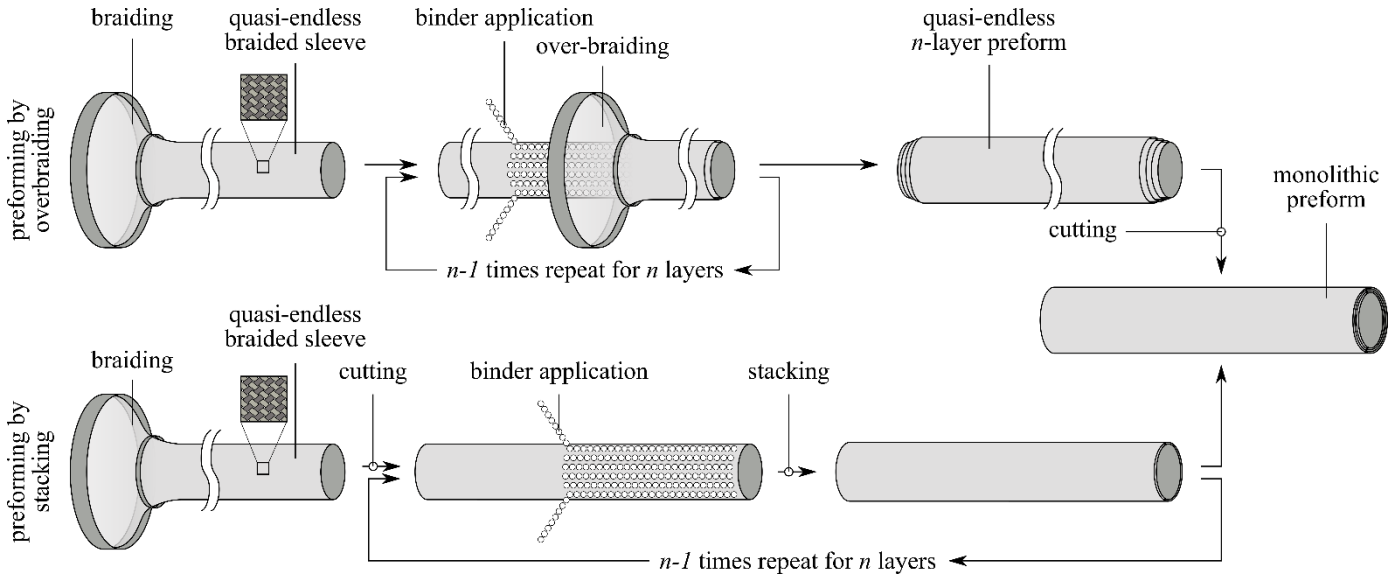

Fig. 2: Comparison of different process routes: preforming by over-braiding and preforming by stacking

- Braiding or over-braiding, which is widely investigated, e.g. in [7]
- Binder application and activation, which has been investigated for rovings in [8], but not successfully applicated for braided preforms. An approach is to store the binder powder in a cylindrical container, which has a conical lower end and a defined opening at the bottom. The binder dispersion is then started by vibration. In first tests, this approach has shown an even dispersion of the binder onto braided sleeves. Based on these first results, the binder application onto a braided sleeve and the activation will therefore be investigated in subsequent studies to find the optimum process parameters.

Hybrid preforming

The above described monolithic preforming is followed by hybrid preforming, where the monolithic preform is draped onto metallic end fittings. The main process steps are shown in Fig. 3 and are described below.

First, the metallic end fittings and the monolithic preform are joined by a linear movement of the fittings towards each other (1). Then, the overlap areas (areas where FRP and metal overlap) are heated by infrared radiators until the binder is melted (2). Subsequently, the preform and the metallic fitting are put into a forming unit (3). Here, silicon membranes are pressurized and therefore expanded as shown in Fig. 3. The membranes press against the preform and consequently drape the fiber layers along the shape of the metallic fitting. When the binder hardens again on cooling, the area between the overlap areas that has not been draped yet, is heated by infrared radiators (4). After the liquefaction of the binder, the preform is elongated by slightly moving the end fittings away from one another. When the binder is hardened, the hybrid preform is finished (5) and may be infiltrated with resin in subsequent process steps.

A machine for producing such a preform has been built and tested. The first result of manufacturing a hybrid preform is shown in Fig. 4. It can be shown, that the fiber layers of the braided preform follow the shape of the metallic element, but there is still a gap between the fiber layers and the metallic fitting. The following challenges can be derived from the first results:

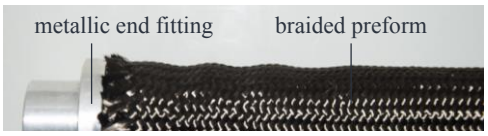

Fig. 4: Manufactured hybrid preform

- As the tool is double shelled, the closing area between both shells leads to wrinkles along the closing line.
- The shape of the membranes has to be optimized in order to drape the monolithic preform onto the end fittings without a gap.

To face these challenges, a finite elements analyses (FEA) of the draping process is necessary, which serves as a process model for the design of the draping.

Such a FEA model consists of the following parts: silicone membranes modeled as hyperelastic shells, the metallic end fitting modeled as a rigid body, and the monolithic preform modeled as a multi-layered coupling of shell and membrane elements. Such a technique to model preforms has first been described by Nishi [9] and has also been taken up by Kärger [10] and Coutandin [11]. In this technique, the shell elements represent the bending behavior of the fiber layer while the membrane elements represent in-plane shear and tension. Multiple of such modeled layer parts form a preform. Between the above described parts, interactions in form of friction play a crucial role.

To build such a FEA model, the first step is to gather the necessary material data which can be put into the model. For the above described model, the following data is needed:

- Bending, shear and tension behavior of the braided, binder-applicated fiber layers in the monolithic preform
- Silicone-to-braided sleeve, fiber-to-fiber and fiber-to-metal friction behavior
- Hyper elastic properties of the silicone.

Except the tension behavior of the used fibers and the elastic behavior of the silicone, which is derived by the material manufacturer, the material data has to be obtained in customized tests. The realization and the results of these tests are described in the following chapter.

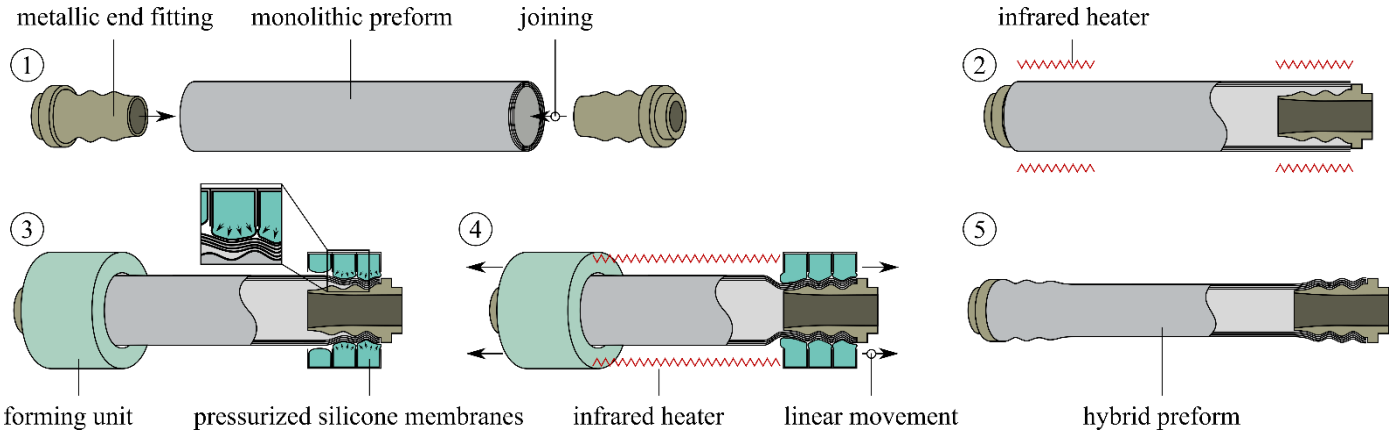

Fig. 3: Hybrid Preforming steps 1 - 5

3. Material Characterization

Shear, bending and friction tests are performed to determine the material properties of the monolithic preform. Due to the geometric similarity of braids and woven fabrics, existing methods for woven fabrics are used for the mechanical characterization of braided hoses. A braided hose with the designation Siltex 7602 made of Toho Tenax HTS 40 carbon fiber rovings (12K, 800tex) is used for the examination.

Fig. 5 shows the geometric structure of a braided hose. By changing the diameter D and the length L of the braided hose, the braiding angle α is adapted to the respective test [7]. Compared to a woven fabric, a braiding angle $\alpha = 45°$corresponds to an unsheared woven fabric.

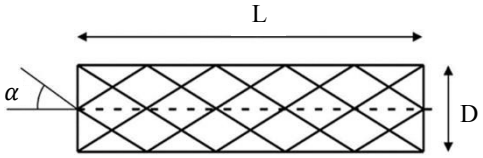

Fig. 5. Geometric structure of a braided hose [7]

The braided hoses are cut in axial direction to produce flat braids. The samples consist of two layers of braid. The braiding axes of both layers point in the same direction. Two percent by weight of EPIKOTE™ Resin 05390 binder is applied between the layers. All tests are performed in an oven at 100 °C (see also [12]). Five measurements are performed per sample configuration.

3.1. Picture Frame Test

The picture frame test is used to examine the shear properties of the monolithic preform. Fig. 6 shows the schematic structure of the experiment.

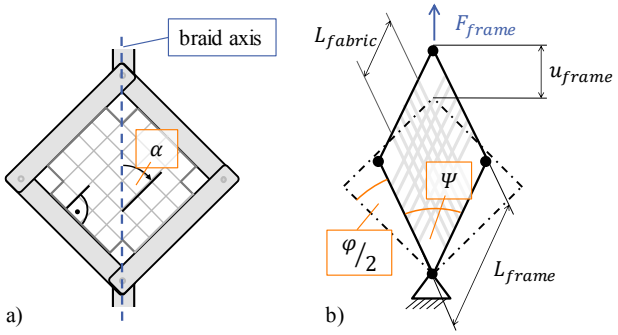

Fig. 6. Picture frame test: a) Orientation of the braided hose; b) Schematic representation of kinematics [13]

A textile sample is clamped into a shearing frame and loaded with a tensile force at opposite corners. This deforms the originally square specimen into a parallelogram [14]. Usually the picture frame test is used to examine woven fabrics [15–18]. The sample size of braids is limited by the diameter. Therefore, a smaller frame is used in comparison to woven fabrics. The frame length of the picture frame is $L_{frame} = 60\ mm$ and the side length of the sample is $L_{fabric} = 40\ mm$. Samples with a braiding angle of 45° are used to characterize the shear properties.

The rovings of the sample are aligned parallel to the shear arms. As a result, the samples are loaded with pure shear [14].

Tests are performed with a crosshead displacement rate of 5 mm/s. During the test, the tensile force and the displacement are measured. The normalized shear force $F_{S,N}$ and the shear angle α are calculated from the displacement and the tensile force according to [16]. The results of the experiment are shown in Fig. 7.

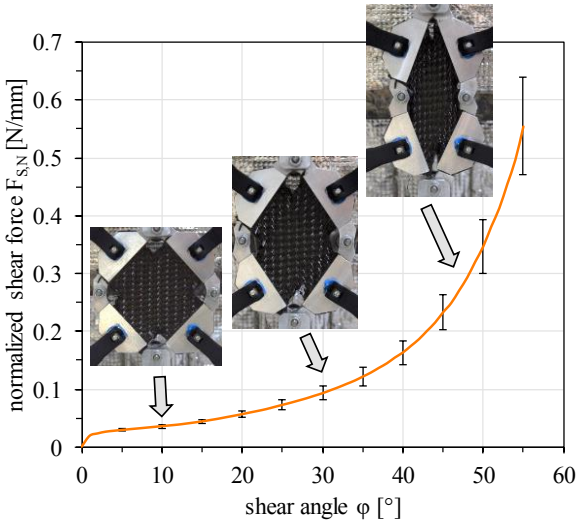

Fig. 7. Normalized shear force $F_{S,N}$ as a function of shear angle φ

The curve can be divided into three sections. In the first section, the shear force is low. It is based on the rigid body rotation of the fiber bundles, which generate friction forces at their intersection points. In the second section the shear force increases. Neighboring fiber bundles come into contact, which leads to a compression of the fiber bundles in transverse direction. In the third section, all fiber bundles are in contact and the maximum compression of the bundles occurs. This causes a large increase in shear force and the braid begins to wrinkle. The shearing behavior of braids is comparable to woven fabrics [17, 19].

3.2. Friction Test

The friction test is used to examine the friction properties of the monolithic preform. All friction tests are based on a similar principle. The friction force between the friction partners is measured while the normal force, velocity and temperature remain constant [13, 20–23].

During draping, friction occurs between braid/braid, braid/membrane and braid/metal. In the following, the friction pairing braid/braid will be discussed. Fig. 8 shows the test setup of the experiment. The friction test consists of a slide and a base plate. A braid is attached to slide and base plate. Weights are used to apply a normal force of $F_N = 42.7\ N$ or a surface pressure of $p = 0.13\ bar$. The braiding axes of both specimens point in the direction of the tensile force. Braided hoses with a braiding angle of $\alpha = 32.5°; 45°$ and $57.5°$ are examined (cf.

Fig. 5). Two percent by weight of binder is applied on the braid on the base plate. The binder is first activated in the oven. Afterwards the slide is placed on the base plate. With a constant speed of 5 mm/s the slide is pulled over the base plate and the resulting friction force F_f is measured.

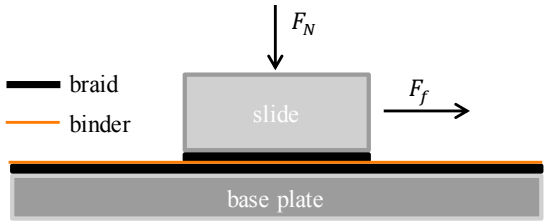

Fig. 8. Schematic setup of the friction test

The friction coefficient μ is calculated according the friction equation $\mu = F_f / F_N$.

Fig. 9 shows the averaged friction coefficient μ as a function of displacement. The static friction coefficient μ_s is the maximum of the friction coefficient curve. The kinetic friction coefficient μ_k results from the average of the measured values in the range from 40 mm to 80 mm. The friction coefficients are depicted in Table 1.

Table 1. Static friction coefficient μ_s and kinetic friction coefficient μ_k

α	μ_H	μ_G
32.5°	0.9	0.71
45°	0.86	0.62
57.5°	0.88	0.64

The change of the braiding angle has minor influence on the static friction coefficient. The intervals of standard deviation of the static friction coefficients overlap. Therefore, the static friction coefficients do not differ significantly. A clear correlation between braiding angle and sliding friction coefficient is not visible.

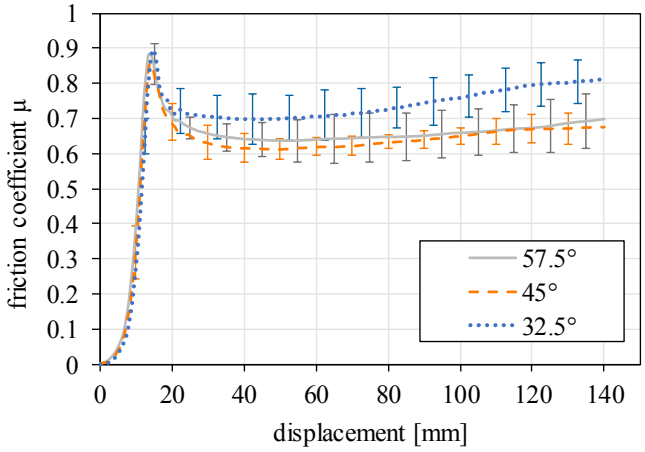

Fig. 9. Friction coefficient μ as a function of displacement

The strong increase of the friction force for small displacements is caused by the pull cord. At the beginning, the cord is not tensioned and the slide does not move.

In this region, the tensile force is lower than the friction force. If the tensile force reaches the maximum friction force (static friction), the slide begins to move.

Therefore, the friction force drops to a constant level (kinetic friction). The slide picks up binder from the base plate during sliding. As a result, the forces in the friction pairing are rising. This causes the force rising at the end of the measurement. In future investigations, the surface pressure will be adapted to 1 bar. This corresponds to the pressure in the membrane during forming.

3.3. Cantilever Test

The cantilever test is used to examine the bending properties of the hybrid preform. Fig. 10 illustrates the setup of the cantilever test. The braid bends under gravity and the overhang length is determined when $\theta = 41.5°$ [24].

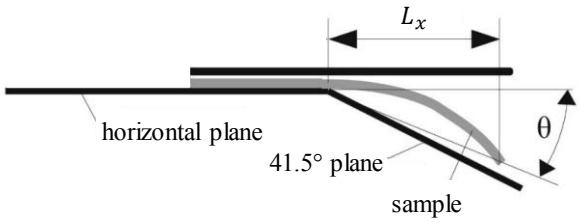

Fig. 10. Schematic setup of the cantilever test [25]

Table 2. Bending stiffness B as a function of braiding angle α

α	$B\ [mNcm^2]$
32.5°	998.13
45°	518.78
57.5°	239.20

In all tests, the braiding axes of the specimens are aligned orthogonally to the bending edge. Braided hoses with a braiding angle of $\alpha = 32.5°; 45°$ and 57.5° are examined (cf. Fig. 5).

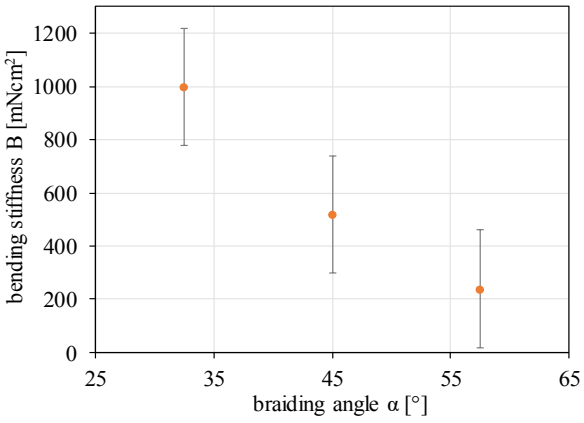

Fig. 11. Bending stiffness B as a function of braiding angle α

The bending stiffness is calculated from the mass of the sample and the overhang length L_x according to [24]. Fig. 11 shows the measured bending stiffness as a function of the

braiding angle. The associated bending stiffnesses are depicted in Table 2.

The bending stiffness decreases with increasing braiding angle. The bending stiffness of the braid can be explained by the orientation of the rovings. Fig. 12 illustrates the orientation of the rovings in relation to the bending edge. Rovings resist the maximum bending load when the fibers are orthogonally aligned to the bending edge. Due to the braiding angle α the rovings deviate from the ideal orientation.

The deviation of the rovings leads to a superposition of torsional and bending stress. As a result, the bending stiffness decreases.

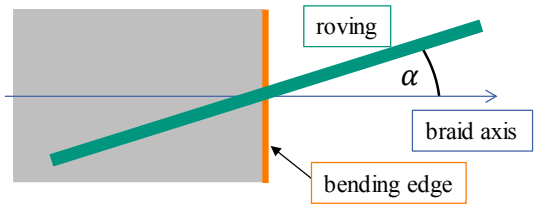

Fig. 12. Orientation of the roving in relation to the bending edge

4. Conclusion

A new process for producing hybrid shafts or rods made of metal and FRP constitutes in the rotational molding process. The basis is a hybrid preform. The process chain for manufacturing a hybrid preform is divided into two steps: monolithic preforming and hybrid preforming. First tests of manufacturing a hybrid preform were conducted. The results showed that the fiber layers of the braided preform follow the shape of the metal element, but there is still a gap between the fiber layers and the metallic fitting.

In the future, a FEA of the draping process will be conducted to produce a form-fit preform. The required material parameters were investigated using picture frame, friction and cantilever test.

Acknowledgements

The process chain for hybrid preforming was developed within the project “FaMeZug”. This project was funded by the Federal Ministry of Economic Affairs and Energy. The simulation model and the material characterization are based on investigations of the project “Beanspruchungsgerechte Gestaltung von Lasteinleitungen für im Schleuderverfahren hergestellte hybride Leichtbauwellen” which is kindly supported by the German Research Foundation (DFG - Deutsche Forschungsgemeinschaft). This project is part of the collaborative research program ‘‘Schwerpunktprogramm 1712’’ of the DFG.

References

[1] Fleischer J, Ochs A *et al.* The future of lightweight manufacturing - production-related challenges when hybridizing metals and continuous fiber-reinforced plastics. Proceedings of International Conference on "New Developments Sheet Metal Forming", 2012, 51–70.

[2] Barfuss D, Grützner R *et al.* Multi-scale structuring for thermoplastic-metal contour joints of hollow profiles. Prod. Eng. Res. Devel. *12*, 2018, 229–238.

[3] Stelzer S, Ucsnik S *et al.* Fatigue behaviour of composite–composite joints reinforced with cold metal transfer welded pins. International Journal of Fatigue *81*, 2015, 37–47.

[4] Fleischer J, Koch S-F *et al.* Manufacturing of polygon fiber reinforced plastic profiles by rotational molding and intrinsic hybridization. Prod. Eng. Res. Devel. *9*, 2015, 317–328.

[5] Koch S-F. Fügen von Metall-Faserverbund-Hybridwellen im Schleuderverfahren: Ein Beitrag zur fertigungsgerechten intrinsischen Hybridisierung, Herzogenrath. Shaker, 2017, 1st edn.

[6] Liebsch A, Kupfer R *et al.* Automated Preforming of Braided Hoses Made of Thermoplast-glass Fiber Hybrid Yarns. Procedia CIRP *66*, 2017, 57–61.

[7] Schillfahrt C, Schledjewski R. Analytical Modelling of Textile Parameters and Draping Behaviour of 2D Biaxial Braided Sleevings. Polymers and Polymer Composites *25*, 2017, 315–326.

[8] Mack J, Mitschang P. Efficient and Flexible Technology for Binder Roving Manufacturing. KMUTNB: IJAST, 2015, 1–8.

[9] Nishi M, Hirashima T. Approach for dry textile composite forming simulation. Proceedings of 19th International Conference on Composite materials (ICCM-19), 2013, 7486–7493.

[10] Kärger L, Galkin S *et al.* Forming optimisation embedded in a CAE chain to assess and enhance the structural performance of composite components. Composite Structures *192*, 2018, 143–152.

[11] Coutandin S, Brandt D *et al.* Influence of punch sequence and prediction of wrinkling in textile forming with a multi-punch tool. Prod. Eng. Res. Devel. *12*, 2018, 779–788.

[12] Coutandin S, Wurba A-K *et al.* Mechanical characterisation of the shear, bending and friction behaviour of bindered woven fabrics during the forming process (submitted). Material Science and Engineering Technology, 2019.

[13] Schirmaier F. Experimentelle Untersuchung und Simulation des Umformverhaltens nähgewirkter unidirektionaler Kohlenstofffasergelege, Karlsruher Institut für Technologie, 2016.

[14] Cherif C. Textile Werkstoffe für den Leichtbau, Berlin, Heidelberg. Springer-Verlag Berlin Heidelberg, 2011.

[15] Lomov SV, Willems A *et al.* Picture Frame Test of Woven Composite Reinforcements with a Full-Field Strain Registration. Textile Research Journal *76*, 2006, 243–252.

[16] Cao J, Akkerman R *et al.* Characterization of mechanical behavior of woven fabrics: Experimental methods and benchmark results. Composites Part A: Applied Science and Manufacturing *39*, 2008, 1037–1053.

[17] Launay J, Hivet G *et al.* Experimental analysis of the influence of tensions on in plane shear behaviour of woven composite reinforcements. Composites Science and Technology *68*, 2008, 506–515.

[18] Gereke T, Döbrich O *et al.* Experimental and computational composite textile reinforcement forming: A review. Composites Part A: Applied Science and Manufacturing *46*, 2013, 1–10.

[19] Boisse P, Gasser A *et al.* Analysis of the mechanical behavior of woven fibrous material using virtual tests at the unit cell level. J Mater Sci *40*, 2005, 5955–5962.

[20] Fetfatsidis KA, Jauffrès D *et al.* Characterization of the tool/fabric and fabric/fabric friction for woven-fabric composites during the thermostamping process. Int J Mater Form *6*, 2013, 209–221.

[21] Allaoui S, Hivet G *et al.* Influence of the dry woven fabrics meso-structure on fabric/fabric contact behavior. Journal of Composite Materials *46*, 2012, 627–639.

[22] Cornelissen B, Sachs U *et al.* Dry friction characterisation of carbon fibre tow and satin weave fabric for composite applications. Composites Part A: Applied Science and Manufacturing *56*, 2014, 127–135.

[23] Sachs U, Akkerman R *et al.* Characterization of the dynamic friction of woven fabrics: Experimental methods and benchmark results. Composites Part A: Applied Science and Manufacturing *67*, 2014, 289–298.

[24] DIN 53362. Testing of plastic films and textile fabrics (excluding nonwovens), coated or not coated with plastics: Determination of stiffness in bending - Method according to Cantilever.

[25] Bilbao E de, Soulat D *et al.* Experimental Study of Bending Behaviour of Reinforcements. Exp Mech *50*, 2010, 333–351.